ChemComm

Accepted Manuscript

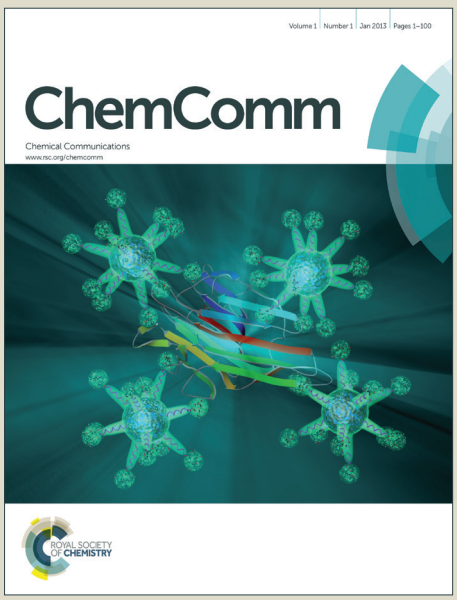

ROYAL SOCIETY OF CHEMISTRY

www.rsc.org/chemcomm

Cite this: DOI: 10.1039/c0xx00000x

www.rsc.org/xxxxxx

ARTICLE TYPE

Self-assemblies of Amphiphilic Homopolymers: Synthesis, Morphology Studies and Biomedical Applications

Jin Zhang,[a] Kelan Liu,[a] Klaus Müllen[b] and Meizhen Yin*[a]

Received (in XXX, XXX) Xth XXXXXXXXX 20XX, Accepted Xth XXXXXXXXX 20XX

DOI: 10.1039/b000000x

The need for a simplified access to supramolecular assemblies with enhanced tenability has led to the development of amphiphilic homopolymers (APHPs). This feature article highlights recent advances and future trends in APHP design, self-assembly, and biomedical applications. APHP self-assemblies are prepared by two different routes: the "monomer-induced" method, which polymerizes functional amphiphilic monomers into micelles and inverse micelles, and the "hydrophobic-group-induced" method, which uses the non-covalent interaction provided by large hydrophobic endgroups. Special emphasis is paid to unimolecular polymeric micelles (UPMs) which are formed from core-shell APHPs and which consist of a hydrophobic/hydrophilic core coated with a polymer shell. The self-assembled supramolecular structures hold promise for various biomedical fields, including living cell transport, fluorescence labelling, protein sensing and extraction, DNA detection, and drug loading and release.

1. Introductions

Macromolecular self-assembly (MSA), which has emerged in the 1970s, aims at constructing increasingly complex structures at varying length scales by utilizing non-covalent interactions of simple macromolecular building blocks. Due to the well-defined structure and relatively narrow molecular-weigh distribution, block copolymers play an important role in the field of MSA. In the 1990s, research toward MSA became relatively mature after many desirable morphologies of block copolymers had been obtained and the relationships between the morphology and copolymer parameters had been determined by theoretical studies.[1-8] Amphiphilic block copolymers are known to self-assemble into a range of nanostructures such as micelles, cylinders, vesicles, large compound micelles, jellyfish, and worm-like structures.[9-11] Yin, Müllen, *et al.*, reported self-assemblies based on poly(2-hydroxyethyl methacrylate)-block-poly(styrene) with solvent dependent morphology.[12] Zhang and Eisenberg summarized the effects of chemical structure, hydrophobic/hydrophilic ratio, concentration, temperature, and environment.[13] Polymer self-assemblies have enhanced stabilities and lowered critical aggregation concentrations (CACs) and thus have found promising applications in fields ranging from drug delivery to templates for TiO_2 films.[14, 15-22]

Unlike the synthesis of block copolymers, that of homopolymers needs only one step, and supramolecular assemblies with enhanced tenability can be achieved easily. For the self-assembly of block copolymers in solution, the immiscibility of either one of the blocks in a given solvent or their mutual incompatibility has been reported as the driving force. However, the main driving force within the self-assembling of homopolymers rests upon intramolecular phase separation and non-covalent interactions. These non-covalent interactions comprise electrostatic forces, π-π stacking, charge-transfer, and hydrogen bonding. In this review, we describe self-assemblies from amphiphilic homopolymers (APHPs) with special focus on their synthesis, morphology studies, and biological applications.

2. Synthesis and self-assemblies of APHPs

Two distinct strategies have been reported for the preparation of homopolymer self-assemblies: the "monomer-induced" method and "hydrophobic-group-induced" method. In the former, the self-assemblies of homopolymers are formed by the polymerization of specially designed amphiphilic monomers. In the latter, the self-assembling of hydrophilic homopolymers results from the non-covalent interaction provided by large hydrophobic endgroups. The most obvious difference between the two approaches is the structure of the APHP. In the "monomer-induced" method, the monomer unit encodes the amphiphilic properties. After polymerization, the polymer contains the hydrophobic part and hydrophilic part in each unit.[23-30] The "hydrophobic-group-induced" APHPs is synthesized by atom transfer radical polymerization (ATRP) and addition-fragmentation chain transfer polymerization (RAFT) , in which the ATRP initiator or RAFT agent serves as a special hydrophobic group and the homopolymer acts as the hydrophilic moiety. Here, we defined the hydrophobic part as a single hydrophobic group or a well-defined hydrophobic dendrimer.

2.1 "Monomer-induced" method

During the design of the monomer, all kinds of non-covalent interactions should be taken into consideration. Non-covalent bonding significantly depends on the environment (e.g., the polarity of the solvent, pH,[31] and temperature[32]), thus offering the opportunity for external control of the self-assembling process. In other words, the system is responsive and can communicate with its environment. Therefore, the design of functional hydrophilic and hydrophobic endgroups is essential, which allows great control over the formation of supramolecular assemblies. Table 1 lists the amphiphilic monomers reported recently. Here we will mainly discuss how the structure of the monomer influences the self-assembly behavior.

Table 1 Structures and features of amphiphilic monomers

Structure	Characteristic	Morphology	Polymerization	Ref.
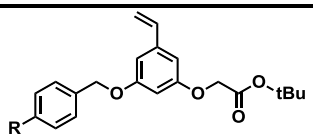	Hydrophilic part: protected functional carboxylic acid group Hydrophobic part: benzyl group	Micelles-type assembly Inverse micelles-type assembly	NMP	23
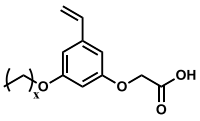 x=5,7,9	Hydrophilic part: carboxylic acid group Hydrophobic part: alkyl chain and benzyl group	Micelles-type assembly Inverse micelles-type assembly	RAFT	
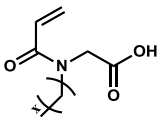 x=5,7,9	Hydrophilic part: secondary amine attached to carboxylic acid Hydrophobic part: alkyl chain	Micelles-type assembly Inverse micelles-type assembly	RAFT	24
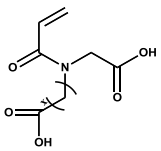 x=5,7,9,15	Hydrophilic part: two carboxylic acids connected by secondary amine Hydrophobic part: alkyl chain	Vesicles-type assembly Reverse micelle-type assembly	RAFT	
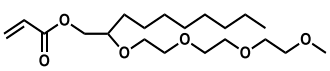	Hydrophilic part: tri(ethylene glycol) monomethyl ether Hydrophobic part: decyl group	Micelle-type assembly Inverse micelles-type assembly	ATRP	25
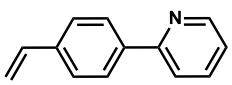	Hydrophilic part: 2-phenyl pyridine Hydrophobic part: vinyl backbone	Vesicles-type assembly	Living anionic polymerization	26
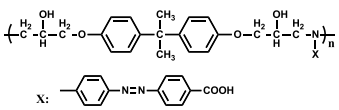 x:	Hydrophilic part: two carboxylic acids and azide Hydrophobic part: benzyl group	Hollow microspheres	Post-polymerization azo coupling reaction	27
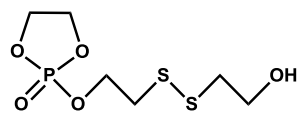	Hydrophilic part: polyphosphate Hydrophobic part: disulfide	Micelles	Ring-opening polymerization (ROP)	28
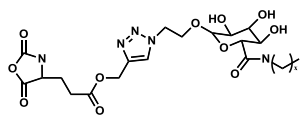 x=3,5,7	Hydrophilic part: homoglycopolypeptide Hydrophobic part: alkyl chain at C-6 position of carbohydrate	Large spherical aggregates	ROP	29
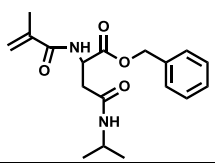	Hydrophilic part: carboxylic acids and the isopropyl amide group Hydrophobic part: alkyl chain	Vesicles	RAFT	30

Thayumanavan *et al.* synthesized a series of styrene-based and glycine-based monomers.[23,24] They stipulated that the

hydrophilic and the hydrophobic functionalities should be on either side of a scaffold so that the monomer was facially amphiphilic. The design strategy was that the relative placement of these functionalities should facilitate the phase segregation of the amphiphilic moieties within the polymer assembly. Thus, the APHP assembled into a micelles-type structure (**Figure 1**) in water, in which the hydrophilic carboxylic acid groups were exposed to the bulk solvent and the hydrophobic part was tucked in the interior of an assembly. Similarly, an inverted micelle-type structure (**Figure 1**) would be expected in apolar solvents, in which the locations of the functional groups were reversed. The environment of the core of the micelles formed by an APHP was more rigid and confined than that of the micelles formed from diblock amphiphilic copolymers and small molecular surfactants.

The polymer self-assembly was changed by the functionalization of other carboxylic acid groups within glycine-based monomers. Here, one of the carboxylate moieties was located in the exterior while the other carboxylate was located in the water-filled interior of the vesicles-type assemblies (**Figure 1**). By changing the solvent, the long alkyl chains could bend to form reverse micelle-type assemblies (**Figure 1**), which consisted of a hydrophobic corona and a hydrophilic core. The chains fold upon increasing their lengths. Thereby, they formed micelle-type assemblies with a hydrophobic corona tucked in the hydrophilic carboxylic acid moieties. Moreover, when two hydrophilic head groups linked by a long hydrophobic alkanediyl chain were incorporated into the repeat units of the homopolymer with critical chain length, vesicular assemblies were obtained. The vesicle assemblies were environment-dependent architectures, and the CACs for these polymers were much lower than those for the small molecular building blocks. [33]

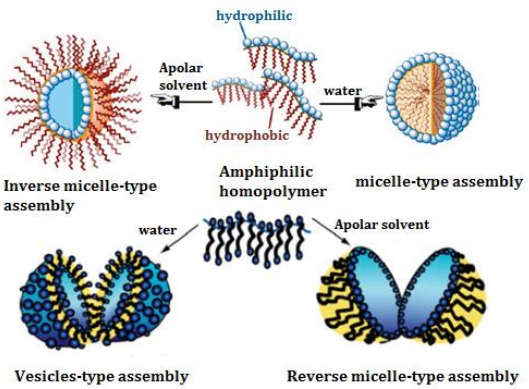

Figure 1 Schematic representation of micelle-type, inverse micelle-type, vesicles-type and reverse micelle-type assemblies. Reproducted with permission from ref. 33 and ref. 24, Copyright (2009, 2006) American Chemical Society.

Huang *et al.* reported ferrocene-containing homopolymer **1** (**Figure 2**) and studied it's self-assembly behavior. [34] The ferrocene-containing monomers consisted of both ferrocene and carboxylic acid formed by the sequential hydrolysis. They found large assembled micelles with different morphologies. The self-assemblies contained numerous reverse micelles with hydrophilic islands of carboxyls in the continuous hydrophobic phase of ferrocene-based segments. By increasing the concentration of polymer **1,** spheres, spindles, and connected spindles were observed. Interestingly, the authors discovered that the amount of β-cyclodextrin (β-CD) would affect the morphology of the self-assemblies. By increasing the amount of the β-CD, the diameter of the sphere increased and finally bowl-shaped self-assemblies were observed.

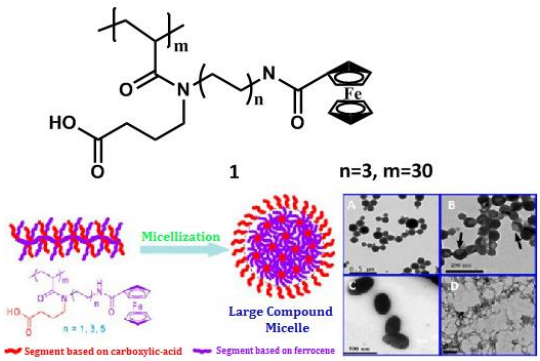

Figure 2 Chemical structure of homopolymer **1**, formation of large compound micelles by **1**, and transmission electron microscopy (TEM) images of micelles formed by **1** with different initial concentrations of (A) 0.2, (B, C) 0.4, and (D) 0.8 mg/ml. Reprinted with permission from ref. 34, Copyright (2013) American Chemical Society.

Wan et al. reported a new approach to creating linear poly(polyoxometalate)s (poly POMs) that combines the advantages of polymers and POM clusters. A POM-containing norbornene monomer was synthesized by linking a Wells-Dawson-type POM with a norbornene derivative. It is known that a POM cluster without counterions has a large ellipsoidal shape, but the repeating unit of the polynorbornenes is relatively small. This difference in size may cause a steric hindrance along the polynorbornene backbone bearing the POM cluster pendants that obstructs the formation of the L-poly(POM)s. Thus, Wan et al. inserted a 12-carbon spacer between the norbornene moiety and the cluster. The resulting homopolymer **2** (**Figure 3**) has controllable molecular weights and a well-defined hybrid structure of an organic polynorbornene backbone with large pendant groups of the nanosized POM clusters. They also demonstrated that homopolymer **2** had advantages in preparing solution-processed thin films to catalyze the oxidation of a sulfide. [35]

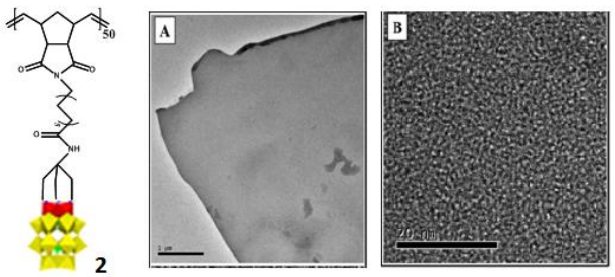

Figure 3 Structures of polymer **2** and TEM images of a thin film of **2** prepared by casting of an acetonitrile solution. Images (A) and (B)

obtained at different magnifications show homogeneous and inhomogeneous morphologies. Reprinted with permission from ref. 35, Copyright (2014) American Chemical Society.

Shivshankar and Shunmugam designed a norbornene-derived thiobarbiturate homopolymer (NDTH) with a hydrophobic alkyl group and a hydrophilic cationic ammonium group based on a poly(norborene) backbone prepared by ring-opening metathesis polymerization (**Figure 4)**. Thus, in an apolar solvent, the NDTH formed Reverse micelle-type assemblies with the hydrophobic norbornene backbone outside. Conversely, in an aqueous medium, the NDTH self-assembled into vesicle-type assemblies with the hydrophilic thiobarbiturate head groups outside. Thus, homopolymer **3** could spontaneously organize into different morphologies in solvent mixtures (tetrahydrofuran/methanol or tetrahydrofuran/water). Here, in both solvent mixtures, the hydrophilic units were densely packed to avoid interaction with the surrounding apolar solvents. Depending on the hydrophilic/hydrophobic balance, **3** underwent two morphology transitions, varying the structure from rods, to bundle micelle-type assemblies, and eventually to cube-like or sphere-like aggregates (**Figure 5**). The thiobarbiturate motifs in **3** provide the connections between the different polymer chains and would also increase the interior viscosity of the aggregates during the formation of cube-like as well as sphere-like aggregates. As a result, **3** self-assembled into different morphologies with a high degree of control and uniformity and solely determined by the properties of the constituent functionality and the nature of the solvents.[36]

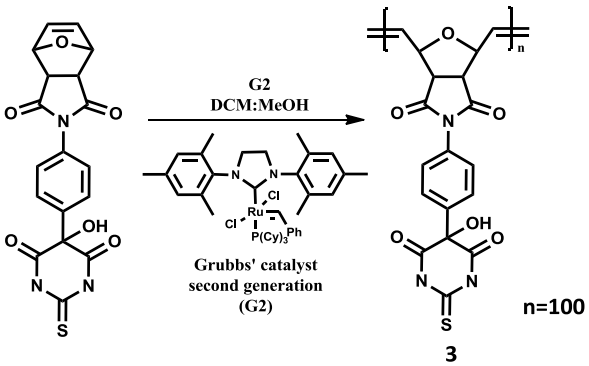

Figure 4 Chemical structure of homopolymer **3.**

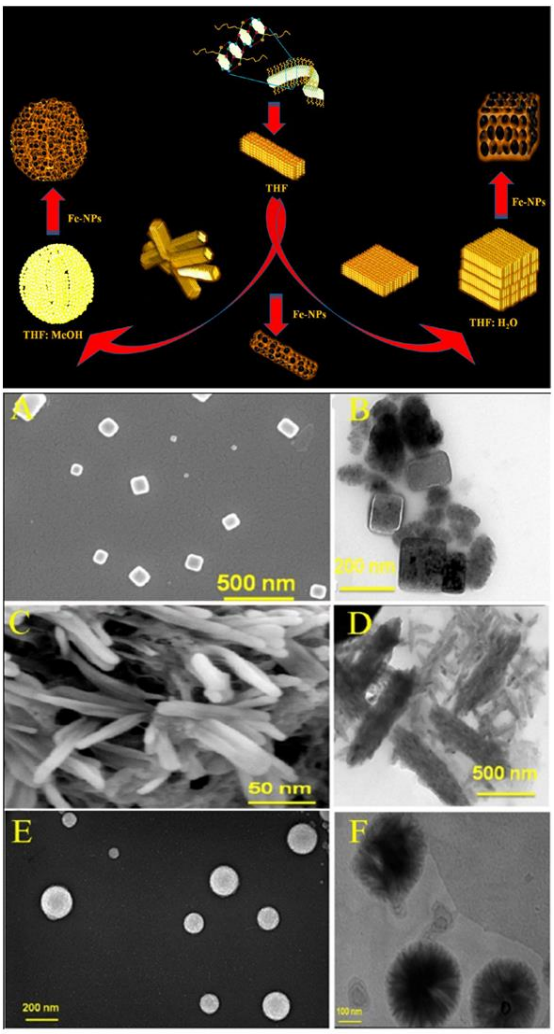

Figure 5 Cartoon representation of overall self-assembly events. A, C, E are SEM images and B, D, F are TEM images of **3** self-assembling in THF/H_2O, THF, and THF/MeOH, respectively. Reprinted with permission from ref. 36, Copyright (2014) American Chemical Society.

Very recently, Du *et al.* proposed that the inter- or intra-polymer hydrogen bonding effect played a key role in the formation of various nanostructures by homopolymer self-assembly.[37] A series of APHPs, poly(2-hydroxy-3-phenoxypropyl acrylate) (PHPPA) with various molecular weights (MWs) was synthesized by a RAFT process utilizing 2-methyl-2-[(dodecylsulfanylthiocarbonyl) sulfanyl] propanoic acid (DDMAT) as CTA and AIBN as initiator. Here, the polar hydroxyl group was introduced into the repeating unit to afford both inter- and intra-polymer hydrogen bonds and served as the hydrophilic part. As shown in **Figure 14**, TEM observations indicated that the PHPPA homopolymer can self-assemble into vesicles and other distinct colloidal structures, such as hydrated large compound micelles (HLCMs), large compound vesicles (LCVs), large compound micelles (LCMs), and even branched cylinders in a binary system, which are sensitively dependent on its (conditions such as solvent properties and solution pH. Here, the inter/intra-polymer hydrogen bonding effect plays a key role in the formation of various nanostructures by homopolymer self-assembly. Additionally, the lack of a large

hydrophilic corona decreases the colloidal stability of homopolymer self-assembly, but the introduction of −COOH as the endgroup increases the negative surface charge and prevents the aggregation of self-assembled nanoparticles.

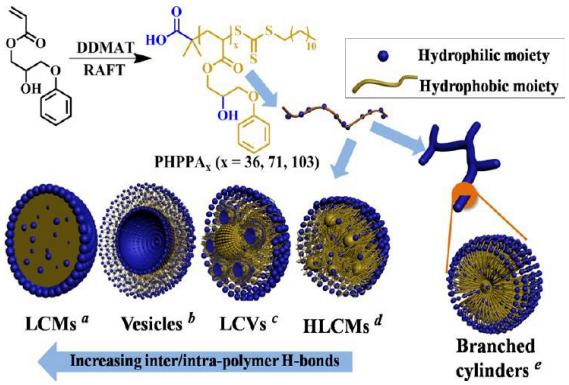

Figure 14 Preparation of PHPPA homopolymers that can self-assemble into a range of nanostructures induced by inter/intra-polymer hydrogen bonding: [a] large compound micelles (LCMs), [b] vesicles, [c] large compound vesicles (LCVs), [d] hydrated large compound micelles (HLCMs), and [e] cross-section model of branched cylinders. Reprinted with permission from ref. 37. Copyright (2013) American Chemical Society.

2. 2 "Hydrophobic-group-induced" method

As we have discussed above, block copolymers can form a range of nanostructures depending on a number of factors.[38, 39] Specially, a suitable hydrophilic-hydrophobic balance in the amphiphilic polymer is required to establish a higher order morphology, and the morphology depends on the dimensionless 'packing parameter'.[40] As a general rule, copolymers with 50 vol.% of the hydrophobic block usually form micelles; copolymers with ~50-66 vol.% of the hydrophobic block usually favor vesicle formation; and those with more than 66 vol.% of hydrophobic block may form vesicles, inverted microstructures, other complex structures such as micelles, and finally macroscopic precipitates.[41] Unlike that from block copolymers, the nanostructure formation from hydrophilic homopolymers does not obey the traditional rules of polymer self-assembly. Due to the non-covalent interactions between the hydrophobic endgroups, the homopolymer can self-assemble into ordered morphologies. In designing the APHPs with hydrophobic groups, both the hydrophilic weight fraction and the subtle effects of hydrophobic endgroups should be taken into consideration.

Sundararajan reported a series of homopolymer **4** with perylene-3,4-dicarboxylic anhydride (PDA) as the hydrophobic core and polysiloxane (PDMS) as the hydrophilic corona (**Figure 6B**).[43] It is known that PDA has two main positions for modification: the peri-position along the long axis of the perylene core and the bay-position along the short axis (**Figure 6A**).[42] The *peri*-positions can be modified in a single step by heating an anhydride and an amine together in a polar solvent at high temperature. Thus, they used the above reactions to modify PDA with PDMS to make amphiphilic polymers. The used chromophore possesses a large planar π-system with a pronounced π-π stacking tendency. Thus, led by π-π stacking of chromophore moiety, the end-capped poly(dimethylsiloxane) **4** spontaneous assembled into vesicles in nonaqueous medium.

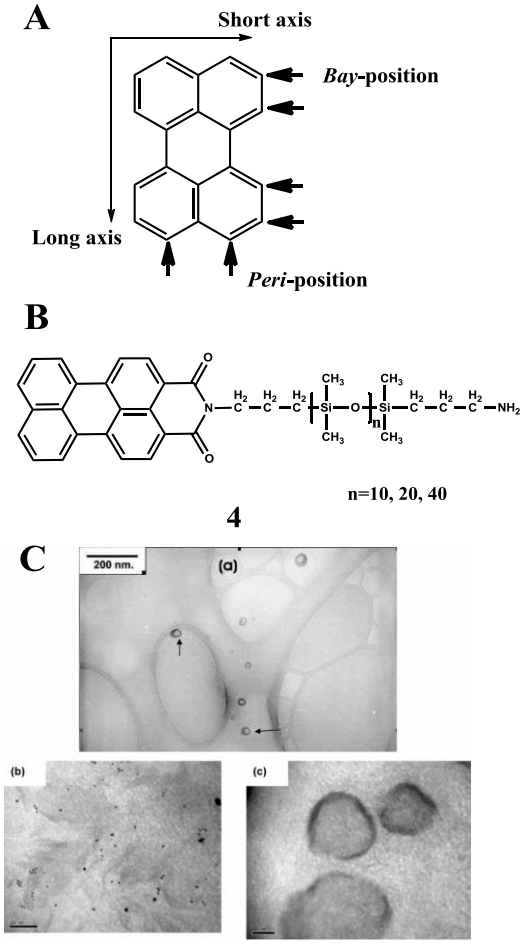

Figure 6 (A)Ways of enlargening the chromophore core; (B) Chemical structure of **4** and (C) TEM image of **4** (a) in $CHCl_3$, C (b, c) cryo-TEM images of **4** in $CHCl_3$. The scale bars in C (b) and C (c) correspond to 100 nm. Reproducted with permission from ref. 43, Copyright (2005) American Chemical Society.

Lin *et al.* obtained temperature-sensitive poly(N-isopropylacryamide) end-capped with rhodamine B (PNIPAAm-RhB).[44] The RhB-ended polymers **5** and **6** were prepared by the amidation of monofunctional and difunctional amine-terminated PNIPAAm chains with RhB (**Figure 7**). Interestingly, the authors found that **5** and **6** can self-assemble into toroidal structures in the chloroform phase at 25 and 60°C, respectively. Compared with the reported toroids of triblock and diblock copolymers, the toroidal structures of **5** and **6** have relatively large ring sizes due to the weak π-π interactions of the RhB moieties. These weak interactions cannot sustain the high bending strains of small rings. When the solution temperature increases to 40 °C, the PNIPAAm chains lose their water solubility, so that the RhB-end-capped PNIPAAm aggregates into particles in the aqueous phase and moves from the aqueous to the chloroform phase.

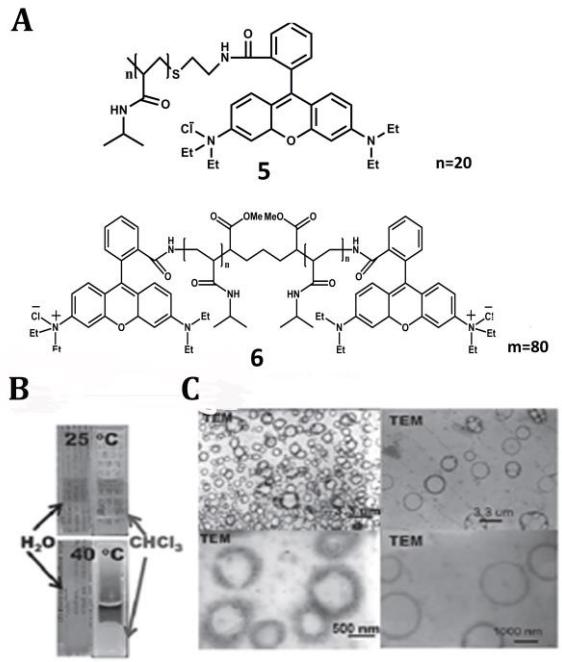

Figure 7 Formation of toroids of RhB-end-capped polymer **5** and **6** (a) the chemical structure. (b) **5** (left) and **6** (right) dissolve in water at 25ºC, and are transferred to the chloroform phase at 40 ºC. (c) TEM micrographs of the **5** (left) and **6** (right) self-assembly in the chloroform phase. Toroidal rings are observed. Reprinted with permission from ref. 44. Copyright (2013) by the Royal Society of Chemistry.

Yin, Müllen, *et al.* reported a specific biological sensor **7** (**Figure 8**) based on a hexa-peri-hexabenzocoronene (HBC) core modified with poly(acrylic acid) chains.[45] The HBC core provided π–π stacking interaction and acted as the hydrophobic part, while the poly(acrylic acid) chain played the role of the hydrophilic part and offered the hydrogen bonding. Driven by the hydrogen bonding and the π–π stacking interaction, the HBC-cored star polymer formed nanofibers in water. Lately, in order to understand the nature of self-assembly involving the interaction between the π–π stack of endgroup moieties and pH-responsive polymers at the micrometer level, Yin's group designed a new kind of pH-responsive perylene-cored APHPs,[46] in which the perylene-3,4-dicarboxylic acid monoimide (PMI) moiety gave rise to a large rigid hydrophobic surface, whereas the flexible poly(amino ethyl methacrylate) (polyAEMA) behaved as a pH-sensitive hydrophilic moiety (**Figure 9**). By adjusting the pH value, polyAEMA transformed from flexible Gaussian coils to aggregated micelles in aqueous solution. At pH<pKa, the polymer behaved as flexible Gaussian coils because of the electrostatic repulsion. At pH=pKa, micelle appeared due to the cooperation of π–π stacking interaction and electrostatic repulsion. At pH>pKa, the micelles aggregated, and after solvent evaporation, flower-like self-assemblies appeared.

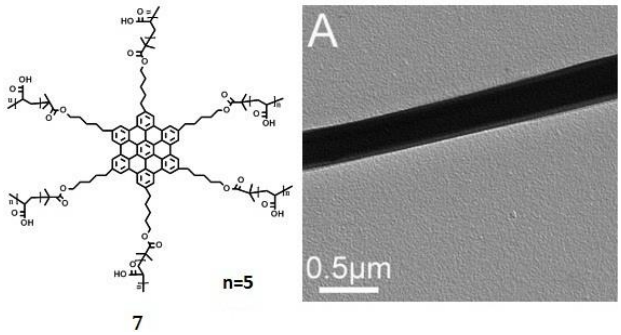

Figure 8 Synthesis of negatively charged HBC-cored homopolymer **8** and TEM image of the microfibers formed when **8** was drop-cast from aqueous solution (1×10^{-5} M) onto a copper grid. Reprinted with permission from ref. 45. Copyright (2009) American Chemical Society.

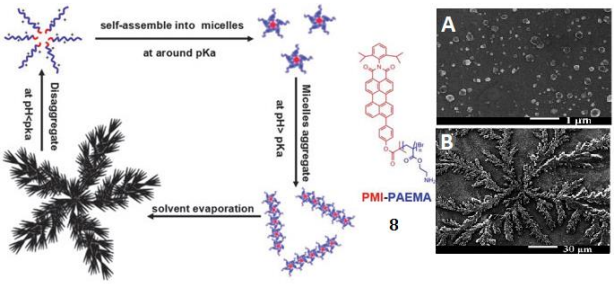

Figure 9 Self-assembly of PMI-based APHP **9** in response to pH variations and the TEM images of the self-assemblies in (A) neutral and (B) alkaline solutions. Reprinted with permission from ref. 46. Copyright (2014) by the Royal Society of Chemistry.

Given the recent advances in controlled radical polymerization (CRP) techniques, the ability to tune the polymer endgroups has now been fully realized, especially for polymers prepared by RAFT,[47-51] in which both the α and the ω chain ends can be incorporated into the chain transfer agent, or introduced after the polymerization by end group modification.[52-54] The effect of the RAFT endgroup on the self-assembly has rarely been considered in the past due to the very small weight fraction of the endgroup compared with that of the polymer chain. However, Davies and co-workers highlighted the selective introduction of two close rings at the ω-terminus of hydrophilic homopolymers.[54] The homopolymers consisted of hydrophilic poly(N,N-dimethylacrylamide) (PDMA) in water bearing two hydrophobic pyrene or cholesterol groups at the ω-terminus (**Figure 12**). Polymersome formation was observed in systems with a remarkably low molar hydrophobic content (typically 6-23 wt %) of either pyrene or cholesterol endgroups. The introduction of a C16 spacer in a bi-ω-pyrenyl-terminated PDMA homopolymer still resulted in the formation of spherical vesicles, although it appeared that the added flexible spacer facilitates full closure of the polymersomes. Increasing the chain end function in the synthesis of a PDMA homopolymer with four pyrenyl units yielded a network-like tubular structure that the authors postulated as being of a bilayer nature.

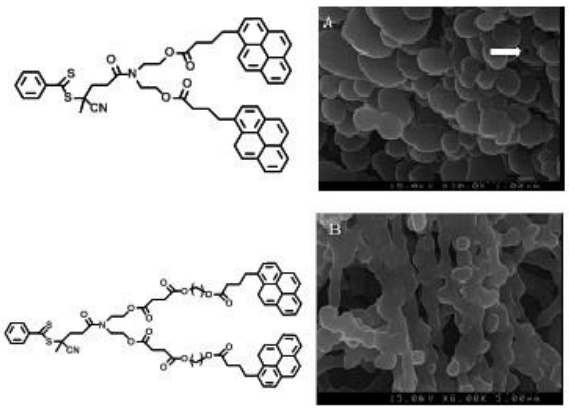

Figure 12 Chemical structures of mono-, bis-, and tetra-functional RAFT CTAs containing pyrenyl moieties in the R group used for (co)polymer synthesis and FE-SEM images of (A) spherical polymersomes and (B) tubular vesicles. Reproducted with permission from ref. 54. Copyright (2013) by the Royal Society of Chemistry.

Du *et al.* demonstrated new classes of homopolymers, which are hydrophilic PNIPAAm and poly(N,N-diethylacrylamide) (PDEA) containing different small hydrophobic endgroups at the α and ω positions, as shown in **Figure 13**.[55] The authors discovered that introducing a second less polar or hydrophobic group at one chain end is essential for the formation of well-defined self-assemblies. Their size was controlled by the polymer concentration and the hydrophobicity of the endgroups.

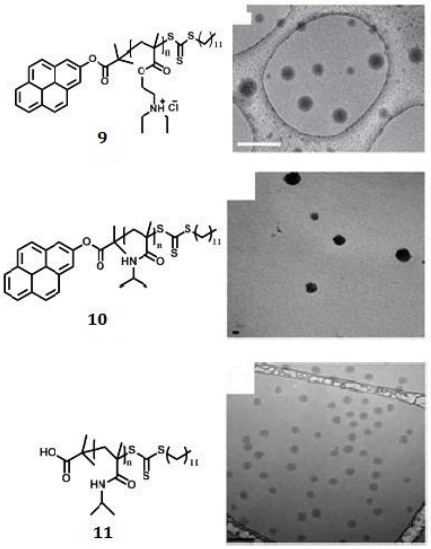

Figure 13 Homopolymers PDEA and PNIPAM (**10**, **11**, and **12)** with different endgroups and TEM images of spherical polymersomes and tubular vesicles. Reproducted with permission from ref. 55, Copyright (2011) by Wiley-VCH.

Recently, the design and controlled fabrication of core-shell macromolecules consisting of hydrophobic/hydrophilic core molecules coated with hydrophilic/hydrophobic polymer shells have aroused much interest in polymer and pharmaceutical research because these core-shell macromolecules usually form unimolecular polymeric micelles (UPMs). The UPMs consist of connected hydrophilic and hydrophobic segments in a single molecule. Therefore, their micellar structure is static rather than dynamic and is maintained at all concentrations and in a variety of solvents, thus offering high structural stability together with small nanosizes, monodispersity, unique spherical shapes, and a number of functional groups at the periphery. Table 2 summarizes typical cores for the core-shell macromolecules based on dendritic star polymers.

Table 2. Typical cores for core-shell macromolecules and their features

Name	Structure	Characteristic	Ref.
Hyperbranched polyglycerols	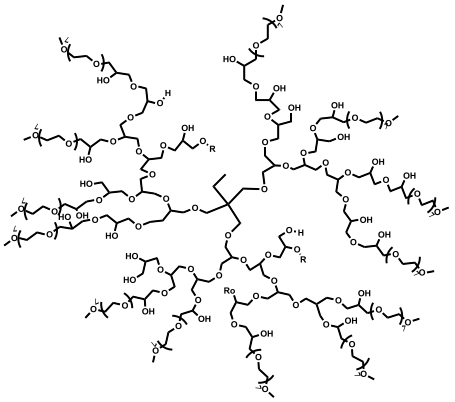	1. Easy to synthesize in a controlled manner with predetermined molecular weights and narrow polydispersity 2. Highly biocompatible, with no evident animal toxicity	56-60

Polyphenylene dendrimer	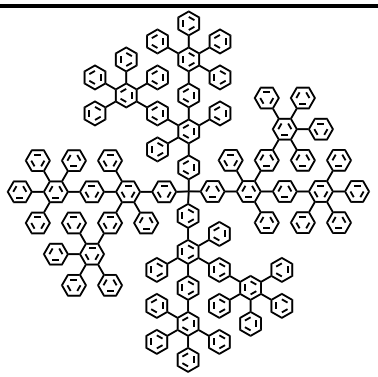	A shape-persistent scaffold	61, 62
Poly(amidoamine) (PAMAM) dendrimers and poly(propylenimine) (PPI) dendrimers	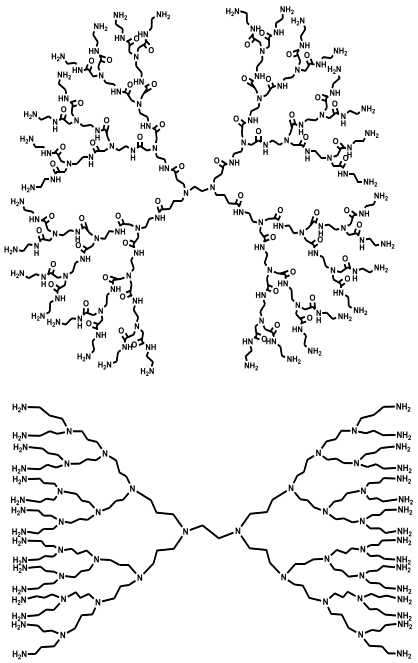	1. Functionalities with terminal groups, such as -NH_2, -OH, -COOH, -$COOCH_3$ 2. Polycationic character with tertiary amines and terminal primary amines	63-76

Yin, Müllen, *et al.* synthesized a series of core-shell structures, in which a central shape-persistent polyphenylene dendrimer served as a scaffold and stabilizer, and outer flexible polymer shells contributed to proton-conducting property.[65, 66] The authors reported a core-shell architecture **12** containing phosphonic acids and studied the self-assembly of such core-shell particles by electrostatic interaction on a modified gold substrate. The atomic force micrograph in **Figure 15** shows many separated globular particles, which appear to be uniformly dispersed, an indication that the core-shell macromolecules formed UPMs. [77]

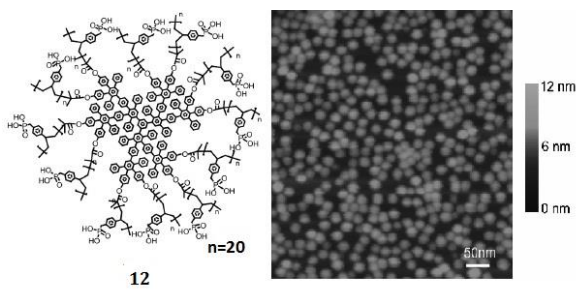

Figure 15 Chemical structure of core-shell macromolecule **13** and the AFM image of a self-assembled film of **13** on modified gold. Reprinted with permission from ref. 78, Copyright (2012) by Wiley-VCH.

Yin, Müllen, *et al.* recently reported a series of fluorescent core-shell macromolecules based on perylene-3,4,9,10-tetracarboxdiimide (PDI) chromophores modified with polyphenylene dendrimers to form a fluorescent shape-persistent cores. The PDI chromophore allowed the detection of multilayer deposition by UV-vis and fluorescence spectral analyses, and the rigid polyphenylene dendrimer was designed to prevent the PDI chromophore from aggregation. A flexible polymer shell enabled the introduction of polar functionalities, for example, amine, hydroxyl or carboxylic acid groups, in order to achieve variation in charges and provided the hydrophilicity. Here, the authors synthesized two kinds of oppositely charged fluorescent core-shell macromolecules **13(c)** and **14(b)**, as shown in **Figure 16**. The core was composed of a rigid polyphenylene dendrimer and PDI chromophore, and the outer shells were flexible cationic or anionic polyelectrolytes that contribute to the water solubility and pH sensitivity. Using small-angle X-ray scattering (SAXS), the authors confirmed

pH-responsive globular UPMs in aqueous solution as a result of the polyelectrolyte nature.[78] The pH-responsive behavior relies on the ionization or deionization of the star polyelectrolytes, which causes a reversible volume phase transition and optical response. In order to detect the formation of multilayer films with the core-shell macromolecules, Layer-by-Layer (LBL) deposition of oppositely charged **13(b)** and **14(a)** was performed in a porous alumina template. During the LBL deposition, polymer chains bearing -NH_2 groups and -COOH groups assembled on the surface of an alumina membrane by electrostatic interactions. **Figure 17** presents the TEM images of a hollow nanotube after the complete removal of the alumina template, and large-scale arrays of fluorescent nanotubes were observed in solution under a conventional fluorescence microscope. [79]

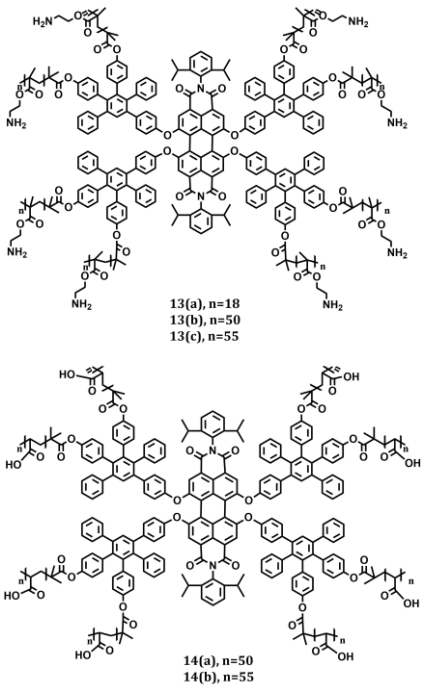

Figure 16 Chemical structures of core-shell macromolecules **14** and **15**.

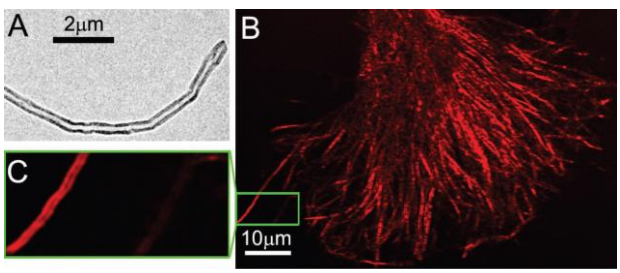

Figure 17 Nanoscale characterizations of fabricated nanotubes by LBL deposition of polymers **14** and **15**. (A) TEM and (B, C) conventional fluorescence microscope images of nanotubes. Reprinted with permission from ref. 79, Copyright (2011) by Wiley-VCH.

3. Biological applications of APHPs

As described previously, APHPs can self-assemble into micelles, vesicles, hollow micelles, bowl shapes, fibers, spindles, and inverse micelle assemblies. Quite naturally, researchers turned their attentions to developing potential applications of these self-assemblies.

3.1 Living cell transport

The visualization and manipulation of cells down to the single molecule level have been widely studied in recent years to understand processes going on in living cells.[80, 81] The synthesis of various chromophores, quantum dots, and fluorescent proteins has provided a deeper understanding of many biological processes such as membrane transport and protein trafficking.[82-86] Particularly, the self-assemblies based on fluorescent polymers are considered as good nanocontainers for cellular transport because they can not only take up and release guest molecules but also monitor the cell transport mechanisms.[87, 88]

Yin, Müllen, *et al.* reported fluorescent core-shell macromolecules **13(a)**, **15**, and **16(a)** with different architectures, charges, and charge densities (**Figure 18**). The fluorescent core-shell macromolecules consisted of a rigid polyphenylene dendrimer core with a hydrophobic PDI chromophore at the center and a hydrophilic flexible polymer shell. The central PDI chromophore allowed the detection of cell transport by fluorescence microscopy, even at the single molecule level, and the first generation (G1, **13(a)**) and second generation (G2, **15** and **16(a)**) polyphenylene dendrimers prevented the PDI chromophore from aggregation in water. The outer shell provided positive charges and water solubility. The investigation of the ability to cross cellular membranes showed that the macromolecules bearing a higher number of polymer chains with less amino groups (positive charges) led to a faster uptake into the cell with no cytotoxicity at the concentrations applied in *in vitro* experiments. [89]

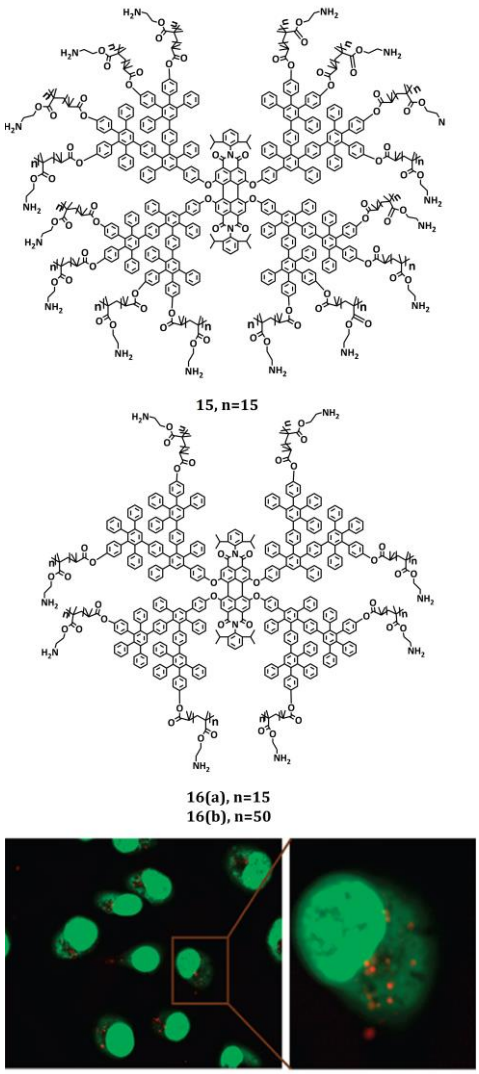

Figure 18 Chemical structure of dendritic core-shell star polymers and penetration of **13(a)** into ECV-304 cells after 15 min. ECV-304 was stained by using a green fluorescence cell tracker, whereas the core-shell macromolecules are shown with a red color. Reproducted with permission from ref. 89. Copyright (2008) American Chemical Society.

3.2 Fluorescence labelling

Fluorescence labelling is widely used in biological studies. It is a process in which a fluorophore is attached to bio-molecules for the detection of proteins or other reporter molecules by a fluorescence microscope, flow cytometer, or fluorescence reading instruments.[90-93] The most commonly labelled molecules are antibodies,[94] amino acids,[95] and peptides[96]. The dynamic processes can be monitored by using dyes as probes.

Yin *et al.* reported that the UPMs (**13(b)**) bearing multiple amines could bind to the highly negatively charged extracellular matrix (ECM) at physiological pH (**Figure 19**) and thus might be applicable to label the ECM of animal tissue. They demonstrated that **13(b)** efficiently stained the tracheal ECM and the staining was much faster than antibody staining procedures, due to the electrostatic interaction between negatively charged ECM components and the positively charged macromolecules **13(b)**.[97]

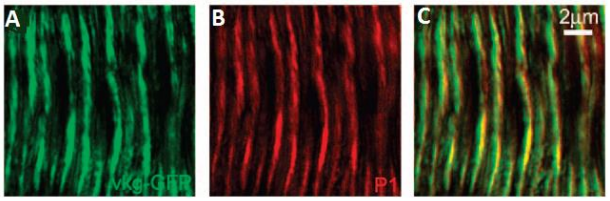

Figure 19 Confocal images of **13(b)** staining (red, central column) of ECM in living tracheal epithelium of vkg-GFP transgenic larvae. (A) GFP fluorescenceis (green). (B) **13(b)** staining (red). (C) Merged channels. Reprinted with permission from ref. 97. Copyright (2008) American Chemical Society.

The authors also found that the UPMs (**14(a)**) bearing multiple carboxylic acid groups could stain the cell nucleus of *Drosophila* by binding to the positively charged nuclear proteins (**Figure 20**). They confirmed that **14(a)** specifically stained the cell nucleus and that the positively charged chromatin histones directly bound with the multiple -COOH groups on the **14(a)** side chains. [98]

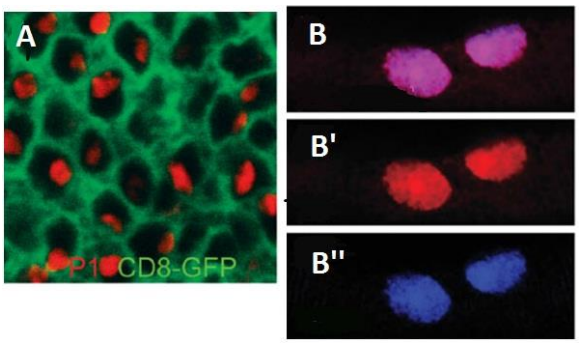

Figure 20 Confocal microscopy images of **14(a)**-stained *Drosophila* larval tissues demonstrate exclusively nuclear **14(a)** localization. (A) Visualization of **14(a)** staining (red) on the cell membrane. The cell membrane is marked by expression of the genetic marker CD8-GFP (green; optical section through the columnar epithelium). (B) **14(a)** fluorescence (red) overlaps with the DNA dye DAPI (blue) in the tracheal squamous epithelium. Single channels are separated in (B') and (B''). DAPI=2-(4-amidinophenyl)-6-indolecarbamidine dihydro-chloride). Reprinted with permission from ref. 98, Copyright (2008) by Wiley-VCH.

3.3 Protein sensing, probing, and extraction

Conjugated polyelectrolytes have been the favorite candidates for fluorescence-based sensing of proteins on account of the inherent fluorescence of the polymer backbone and the water solubility. The likelihood of energy or electron transfer or both from the polymer to the biological analyte, resulting in a change in the fluorescence pattern of the polymer, renders the fluorescent sensing particularly powerful for metalloproteins. Thayumanavan *et al.* synthesized a new class of non-conjugated fluorogenic polymers derived from polystyrene-based APHPs (**Figure 21**).[33] These polymers were shown to form optically clear nanoscale micellar assemblies in water. The authors demonstrated that the fluorescence response from the fluorophore decreased as the concentration of the metalloproteins was increased, whereas a

similar increase in lysozyme concentration had no discernible effect on fluorophore.

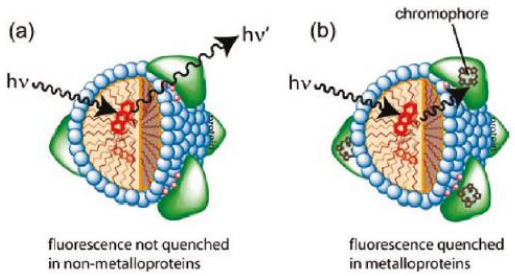

Figure 21 The interaction of polymeric micelles that contain an anthracene unit (a) with non-metalloproteins and (b) with metalloproteins. Reprinted with permission from ref. 33. Copyright (2009) American Chemical Society.

The sensing systems shown in **Figure 21** are based on nonspecific (electrostatic) interactions. For sensing systems to be practical, one needs to ensure high selectivity that can be introduced into a system through lock-and-key-type receptor ligand interactions. Therefore, the authors constructed a new protein sensor array, which carried different fluorescent dyes into the micellar assemblies (**Figure 22**).[99] The non-covalent incorporation of these molecules provided access to a wide variety of different responding systems with high applicability. [96]

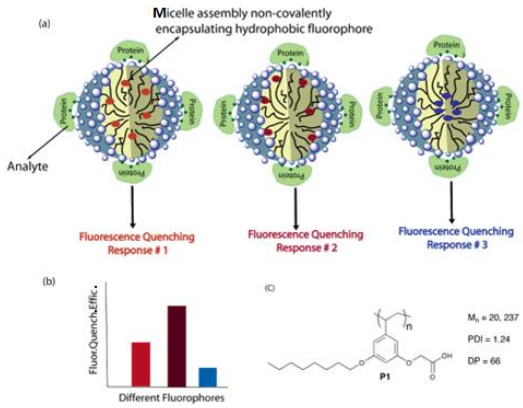

Figure 22 (a) Schematic representation of the differential transducer approaches using APHP micelles. (b) Expected fluorescence quenching response for a hypothetical analyte. (c) Structure of polymer **P1**. Reprinted with permission from ref. 99. Copyright (2007) American Chemical Society.

Yin, Müllen, *et al.* discovered that assembled fibers based on **8** may act as templates for the binding of positively charged peptides by electrostatic interactions. They also demonstrated that if the bound peptides were fluorescein-labelled, the final fibers could be visualized as a dual-color assembly in double-fluorescence imaging (**Figure 23**). [45]

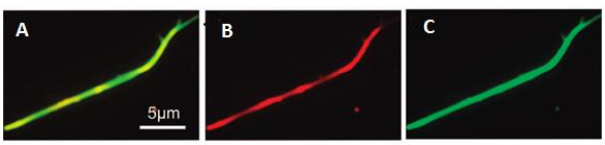

Figure 23 Fuorescence images of negatively charged HBC **7** fibers. Green-fluorescent, positively charged 5(6)-Fam-conjugated peptides bind to the negatively charged fibers to form a dual-color fiber in double-fluorescence imaging (A). Separate channels are shown in (B) (red, HBC **7** fiber) and (C) (green, fiber of 5(6)-Fam). Reprinted with permission from ref. 45. Copyright (2009) American Chemical Society.

Thayumanavan *et al.* synthesized a styrene-based APHP with hydrophilic carboxylate groups. They found that the inverse micelle-type assemblies were able to extract the cationic molecules selectively into the organic phase (**Figure 24**). The results provided evidence that the inverse micelle-type assemblies were capable of selectively recognizing peptides (depending on the isoelectric point). Meanwhile, this technique can also be used for selecting and concentrating peptide fragments from a complex protein digest. Therefore, it indicats that these styrene-based APHPs are suitable for extraction targeted protein from cell lysates. [33, 101]

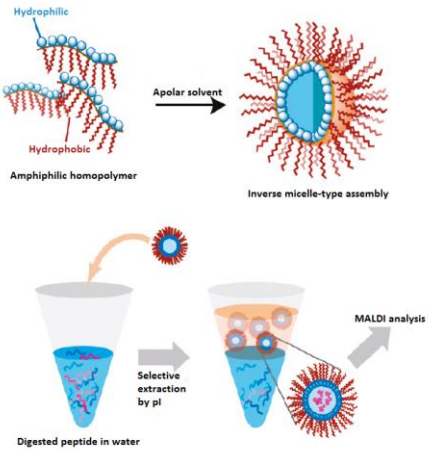

Figure 24 Schematic representation of the selective extraction of complementary peptides from their aqueous solution by using inverse micelles of an APHP. Reprinted with permission from ref. 33. Copyright (2009) American Chemical Society.

3.4 DNA detection, binding, and release

Array-based DNA sensors have become nearly ubiquitous over the past decade, in tandem with the unraveling of the genetic codes of many living organisms. Such sensors have shown great promise in medical diagnosis, biowarfare agent detection, and forensic analysis. The commonly employed substrates, however, have limitations including weak chemical resistance to organic solvents, mechanical instability, and high intrinsic fluorescence. To develop DNA biosensors with suitably functionalized surfaces for DNA immobilization and hybridization thus becomes an important challenge. According to the literature, dendritic star polymers with both dendrimers and star polymers have become suitable candidates for DNA biosensor applications. Because the three-dimensional macromolecular structure of dendritic star polymers provides a stable attachment to DNA and a high binding capacity due to a large number of covalent binding sites of probes, the star polymer chains will increase the limit of detection upon DNA hybridization. [102-106]

Yin, Müllen, *et al.* developed efficient biosensors for DNA

detections, utilizing a new class of ultrathin multilayer films based on dendritic star polymers **17**, **18** and **19** (**Figure 25**).[107] Multilayer thin films were prepared by the alternating adsorption of oppositely charged macromolecules by using the LBL technique. The assembled multilayer films exhibited morphology changes upon post-treatment under different pH conditions. The results of DNA hybridization kinetics demonstrated that these multilayer films provided a stable immobilization of probe DNAs and had similar DNA hybridization kinetics on different surfaces of positive charged films.

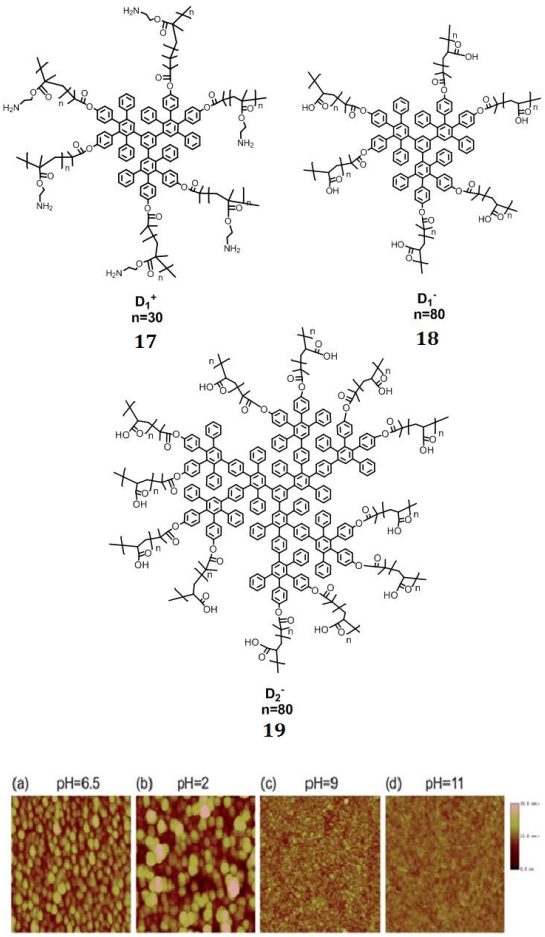

Figure 25 Structures of first- and second-generation oppositely charged dendritic star polymers and AFM images of (**17**/**19**) 8-layer film assembled from **17** solution (at pH 6) and **19** solution (at pH 6.5) before (a) and after 5 min exposure to pH 2 (b), pH 9 (c), or pH 11 (d) aqueous solution. Reprinted with permission from ref. 107. Copyright (2012) by the Royal Society of Chemistry.

The authors also discovered that the oppositely charged fluorescent core-shell macromolecules (**13(b)** and **14(a)**) were UPMs and self-assembled into dual-response fluorescent nanotubes by using the LBL technique in an alumina template. When **13(b)** was deposited as the final layer, the inner -NH_2 surfaces of the outermost layer were protonated under acidic or physiological conditions. Thus, the surfaces were positively charged and interacted with negatively charged DNA through electrostatic forces (**Figure 26**). When **14(a)** was deposited as the final layer, the inner surface of the nanotubes was covered with -COOH groups. By using the amidation reaction to functionalize the carboxylic group with amino-modified single-stranded DNA, a secondary responsive DNA detection was achieved according to the specific hybridization between the above single-stranded probe DNA and its target DNA by base complementarity (**Figure 6 (C)**). [108]

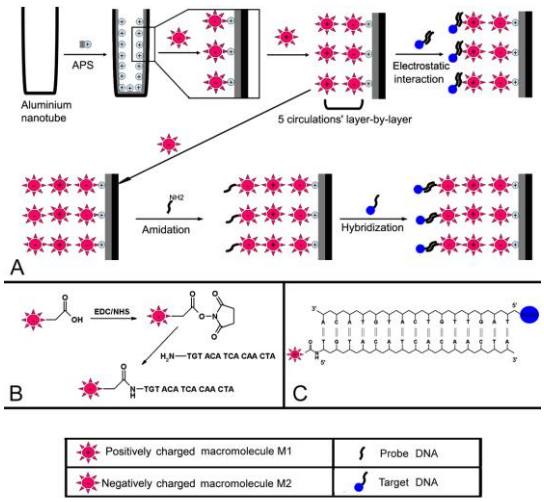

Figure 26 (A) Schematic diagram of the fabrication of fluorescent nanotubes by LBL deposition of oppositely charged **13(b)** and **14(a)**. (B) The activation of -COOH groups with 1-ethyl-3-(dimethylamino)-propylcarbodiimide/N-hydroxysuccinimide (NHS/EDC) and the immobilization (amidation) of amino-modified single-stranded probe DNA. (C) Hybridization of IRD700-labeled target DNA. Reprinted with permission from ref. 108. Copyright (2008) American Chemical Society.

3.5 Drug loading and release

It is well accepted that precise control over the hydrodynamic volume, morphology, chemical composition, and structure of polymers is necessary for a future nanomedicine. [109-115] APHPs have been used in drug loading and release applications, as evidenced by the increasing number of publications in recent years.

As described above, Shunmugam and Sarma reported pH- and lipid- sensitive polymersomes obtained from the self-assembly of polymer **3** (**Figure 27**). The polymersomes were used as a nano-reservoir for the controlled release of doxorubicin (DOXY). These novel polymersomes were capable of loading high drug quantities with a reasonable loading efficiency (about 70% w/w) and of undergoing internalization by living cells. At the mildly acidic pH values of 5.5−6, the drug release from the polymersomes of **3** was significantly accelerated. [116]

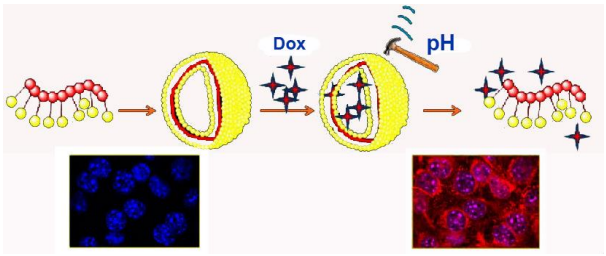

Scheme 27 Cartoon representation of stimuli-responsive drug release and confocal laser scanning microscopy pictures for the uptake of **3**-DOXY. Reprinted with permission from ref. 116. Copyright (2012) American Chemical Society.

Yan et al. synthesized an amphiphilic hyperbranched homopolymer with alternating hydrophobic disulfide and hydrophilic polyphosphate segments along the highly branched structure by self-condensing ring-opening polymerization of the monomer consisting of both hydrophobic disulfide and hydrophilic phosphate moieties (**Figure 28**). The reported amphiphilic hyperbranched homopolymer was a novel precursor for molecular self-assembly and the final micelles possessed a core-shell structure. Here, the disulfide part formed the hydrophobic core and the hydrophilic polyphosphate segments acted as the shells. Furthermore, the micelles were stable in aqueous solution, while they exhibited smart responses in a reductive environment due to the rupture of the disulfide. With the help of hyperbranched polyphosphate micelles, hydrophobic anticancer drugs could be rapidly and efficiently transported into the nuclei of tumor cells and showed enhanced inhibition of cell proliferation (**Figure 28**).[28]

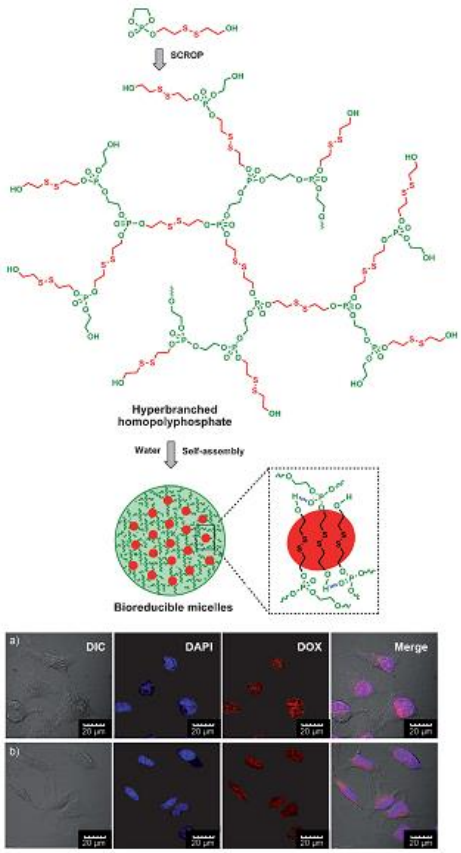

Figure 28 Schematic representations of the self-assembled micelles and representative confocal laser scanning microscopy images of Hela cells incubated with DOX-loaded $HPHDP_1$ micelles for 1 h (a) with or (b) without pretreatment with 10 mm glutathione monoester for 2 h (cell nuclei were stained with DAPI). DIC (differential interface contrast); DAPI: (2-(4-amidinophenyl)-6-indolecarbamidine dihydrochloride). Reprinted with permission from ref. 28, Copyright (2011) by Wiley-VCH.

Du *et al.* proposed a homopolymer vesicle of low cyclotoxicity with a distinct gradient bilayer membrane based on the self-assembly of the hydrophilic and charged homopolymer poly(2-(2-ethoxyethoxy)ethyl acrylate) (PEEA) in a THF-water mixture (**Figure 29**). The PEEA was synthesized from 2-(2-ethoxyethoxy)ethyl acrylate by RAFT polymerization by utilizing 2-methyl-2-[(dodecylsulfanylthiocarbonyl)sulfanyl] propanoic acid (DDMAT) as chain transfer agent (CTA). Here, the increasing degree of hydrogen bonding between the oligo(ethyleneoxy) side chains (OEs) and water supports the assembly of the PEEA homopolymer into a gradient bilayer membrane. The α-COOH groups in the CTA are expressed on both sides of the vesicle membrane to stabilize the vesicle, while the hydrophobic ω dodecyl groups in the CTA are located at the centre of the membrane, forming the densest part of the vesicle membrane. The homopolymer vesicles showed a dynamic aggregation behavior, a thermo-responsive zeta potential, and dispersibility in aqueous solution, thus allowing potential applications in anti-cancer drug delivery. Therefore, the authors encapsulated an anti-cancer drug DOX into the PEEA vesicles, resulting in high drug loading efficiency and sustained drug

release. [117]

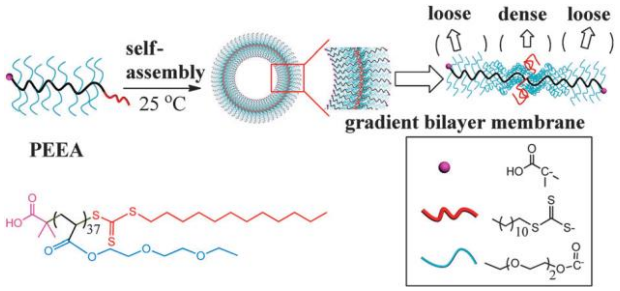

Scheme 29 PEEA homopolymer vesicles with a gradient bilayer membrane. Reprinted with permission from ref. 117. Copyright (2013) by the Royal Society of Chemistry.

MRI (magnetic resonance imaging)-guided drug delivery can be used to monitor the delivery of theranostic nanoparticles to the target sites and to provide information on the therapeutic response of a tumor by real-time monitoring. Haam *et al.* prepared herceptin-modified, pH-sensitive drug-delivering magnetic nanoparticles (HER-DMNPs). The α-pyrenyl-ω-carboxyl poly(ethylene glycol) (Py-PEG-COOH), which was functionalized by the antibody herceptin (anti HER2/neu), encapsulated MR (magnetic resonance)-sensitive $MnFe_2O_4$ nanocrystals (MNCs) modified with doxorubicin (DOX) by the nanoemulsion method. DOX and the pyrene groups can be bound together by a strong π–π interaction for drug encapsulation at neutral pH (≈7.4), and the protonation of DOX under the intracellular acidic conditions of cancer cells (pH < 5) can cause its release by weakening this π-π interaction (**Figure 30**). The authors described the targeted delivery of HER-DMNPs to HER2/neu over-expressed breast cancer cells as an example of a sophisticated cancer therapy based on MRI. [118]

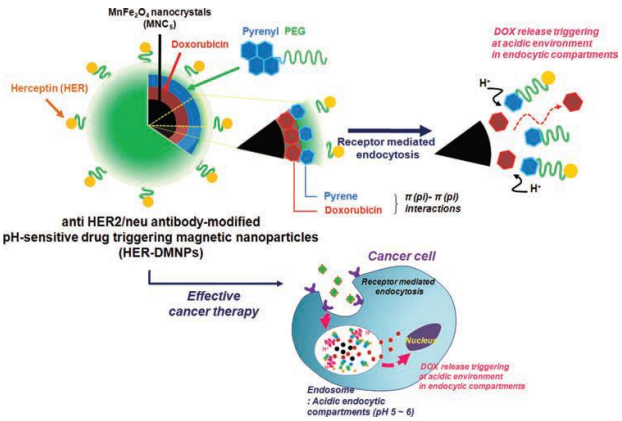

Figure 30 Schematic illustration of pH-sensitive drug-releasing magnetic nanoparticles modified with the antibody anti HER2/neu (HER-DMNPs) for cancer therapy based on MRI. Reprinted with permission from ref. 118, Copyright (2011) by Wiley-VCH.

4. Conclusions and perspectives

APHPs have recently emerged as promising candidates for macromolecular self-assembly and use in biomedical applications. In this feature article, two major methods for fabricating APHP self-assemblies have been described in detail. The "monomer-induced" self-assemblies, which are polymerized with functional amphiphilic monomers, form micelles and inverse micelles by intramolecular phase separation and can be used for drug delivery and protein extraction. The "Hydrophobic-group-induced" APHPs, which comprise a large hydrophobic group and stimulus-responsive hydrophilic polymers, tend to assume a variety of structures by the introduction of non-covalent interaction (e.g., π-π stacking and hydrogen bonding) into the self-assemblies. Especially, the UPMs formed from core-shell macromolecules, which consist of a hydrophobic core coated with polymer shells, have been widely used for biomedical purposes. Such UPMs that are coated with positive/negative charges and water-soluble homopolymers can be used in living cell transport and drug delivery. By introducing fluorophors into these homopolymers, these homopolymers can be applied in labelling, sensing, and in detecting biomolecules such as nucleic acids, proteins, and cells.

Unlike amphiphilic block copolymers, the chemical structures of APHPs are readily designable and tunable. Moreover, the selected examples in this article demonstrate that homopolymers are easy to self-assemble into inverse micelles and vesicles with low CMCs and high tenability because the hydrophobicity can originate from both the polymer backbone and the side chains. Especially, the direct synthesis of a hydrophobic/hydrophilic core coated with a polymer shell affords core-shell macromolecules, which form stable micelles at all concentrations and in diverse solutions.

Although these achievements are encouraging, there are still many challenging issues that need to be resolved. First, progress in the design and development of drug delivery based on highly target specific APHPs is needed. Up to now, only cell-targeting agents (e.g., antibodies, folic acids, and peptides) using block copolymers as carriers have been reported.[119] The chemical structures of APHPs are particularly versatile. This offers the promise to design new amphiphilic monomers with cell-targeting agents or introduce cell-targeting agents into hydrophobic-groups. Second, the self-assemblies of APHP could be simultaneously functionalized with other properties in addition to environmental responsiveness. Since internal stimuli in complex biological systems are inherently difficult to control, multiple-stimuli-responsive systems that can be triggered by both internal and external stimuli will synergistically enhance therapeutic selectivity. Therefore, the development of APHP self-assemblies incorporating multiple-stimuli-responsive elements will result in improved control and specificity of therapeutic agents. Moreover, polymer-based nanomaterials, which are superior to inorganic nanoparticles, are promising for biomedical applications. In general, a polymer-based theranostic material is composed of three main components: (i) a polymer component that offers stabilization and biocompatibility, (ii) a therapeutic agent (e.g., small-molecule drug and siRNA), and (iii) an imaging agent (e.g., MRI contrast agent, radionuclide, and fluorophore). Thus, there is a great demand for multiple-stimuli-responsive design. Lastly, the development of new amphiphilic monomers is

necessary. In addition to the biomedical applications listed in this article, amphiphilic monomers used in other fields, such as biological recognition, separation, bio-thermal and chemical sensors, also need to be explored. Future studies will be focused not only on APHPs with more complicated morphologies, but also on understanding the complex mechanisms of APHP self-assembly.

Acknowledgements

This work was financially supported by the National Natural Science Foundation of China (21174012, 51103008 and 51221002) and the Beijing Natural Science Foundation (2142026).

Notes and references

[a] State Key Laboratory of Chemical Resource Engineering, Key Laboratory of Carbon Fiber and Functional Polymers of Ministry of Education, Beijing Laboratory of Biomedical Materials, Beijing University of Chemical Technology, 100029 Beijing, China.
E-mail: yinmz@mail.buct.edu.cn
[b] Max-Planck-Institute for Polymer Research, Ackermannweg 10, 55128 Mainz, Germany

† Electronic Supplementary Information (ESI) available: Synthesis procedures and material characterizations. See DOI:10.1039/b000000x/

1. S. Motala-Timol, D. Jhurry, J. Zhou, A. Bhaw-Luximon, G. Mohun, H. Ritter, *Macromolecules*, 2008, **41 (15)**, 5571-5576.
2. S.-C. Chan, S.-W. Kuo, C.-H. Lu, H.-F. Lee, F.-C. Chang, *Polymer*, 2007, **48 (17)**, 5059-5068.
3. P. H. Tung, S. W. Kuo, S. C. Chan, C. H. Hsu, C. F.Wang, F. C. Chang, *Macromol. Chem. Phys.*, 2007, **208 (16)**, 1823-1831.
4. O.Colombani, M. Ruppel, F. Schubert, H. Zettl, D. V. Pergushov, A. H. Müller, *Macromolecules*, 2007, **40 (12)**, 4338-4350.
5. O.Colombani, M. Ruppel, M. Burkhardt, M. Drechsler, M. Schumacher, M. Gradzielski, R. Schweins, A. H. Müller, *Macromolecules*, 2007, **40 (12)**, 4351-4362.
6. P. Bhargava, Y. Tu, J. X. Zheng, H. Xiong, R. P. Quirk, S. Z. Cheng, *J. Am. Chem. Soc.*, 2007, **129 (5)**, 1113-1121.
7. L. Liu, X. Gao, Y. Cong, B. Li, Y. Han , *Macromol. Rapid Commun.*, 2006, **27 (4)**, 260-265.
8. J.-F.Gohy, S. Creutz, M. Garcia, B. Mahltig, M. Stamm, R. Jérôme, *Macromolecules*, 2000, **33 (17)**, 6378-6387.
9. J. Du and Y.Chen, *Angew. Chem. Int. Ed.*, 2004, **43 (38)**, 5084-5087.
10. J. Du, Y. Tang, A. L. Lewis, S. P. Armes, *J. Am. Chem. Soc.*, 2005, **127 (51)**, 17982-17983.
11. A. Blanazs, J. Madsen, G. Battaglia, A. J. Ryan, S. P. Armes, *J. Am. Chem. Soc.*, 2011, **133 (41)**, 16581-16587.
12. M. Yin, R. Bauer, M. Klapper, K. Müllen, *Macromol. Chem. Phys.*, 2007, **208 (15)**, 1646-1656.
13. M. Yin, Y. Cheng, M. Liu, J. S. Gutmann, K. Müllen, *Angew. Chem. Int. Ed.*, 2008, **120 (44)**, 8528-8531.
14. D. E. Discher and A. Eisenberg, Science, 2002, **297 (5583)**, 967-973.
15. W. Chen, F. Meng, R. Cheng, Z. Zhong, *J. Controlled Release*, 2010, **142 (1)**, 40-46.
16. Q. Yan, R. Zhou, C. Fu, H. Zhang, Y. Yin, J. Yuan, *Angew. Chem. Int. Ed.*, 2011, **123 (21)**, 5025-5029.
17. J. W. Szostak, D. P. Bartel, P. L. Luisi, *Nature*, 2001, **409 (6818)**, 387-390.
18. R. Roodbeen and J. van Hest, *Bioessays*, 2009, **31 (12)**, 1299-1308.
19. T. Alpermann, K. Rüdel, R. Rüger, F. Steiniger, S. Nietzsche, V. Filiz, S. Förster, A. Fahr, W. Weigand, *Origins Life Evol. Bio.*, 2011, **41 (2)**, 103-119.
20. T. L. Poulos, *Nat. Prod. Rep.*, 2007, **24 (3)**, 504-510.
21. J. Du, Y. Tang, A. L. Lewis, S. P. Armes, *J. Am. Chem. Soc.*, 2005, **127 (51)**, 17982-17983.
22. X. Wan, T. Liu and S. Liu, *Biomacromolecules*, 2011, **12 (4)**, 1146-1154.
23. S. Basu, D. R. Vutukuri, S. Shyamroy, B. S. Sandanaraj, S. Thayumanavan, *J. Am. Chem. Soc.*, 2004, **126 (32)**, 9890-9891.
24. E. N. Savariar, S. V. Aathimanikandan and S. Thayumanavan, *J. Am. Chem. Soc.*, 2006, **128 (50)**, 16224-16230.
25. Y. Wang, A. M. Alb, J. He, S. M. Grayson, *Poly. Chem.*, 2014, **5 (2)**, 622-629.
26. M. Changez, N. G. Kang, C. H. Lee, J. S. Lee, *Small*, 2010, **6 (1)**, 63-68.
27. N. Li, G. Ye, Y. He, X. Wang, *Chem. Commun.*, 2011, **47 (16)**, 4757-4759.
28. J. Liu, W. Huang, Y. Pang, P. Huang, X. Zhu, Y. Zhou, D. Yan, *Angew. Chem. Int. Ed.*, 2011, **123 (39)**, 9328-9330.
29. V. Dhaware, A. Y. Shaikh, M. Kar, S. Hotha, S. Sen Gupta, *Langmuir*, 2013, **29 (19)**, 5659-5667.
30. C. Luo, Y. Liu and Z. Li, *Macromolecules*, 2010, **43 (19)**, 8101-8108.
31. X. Jiang, C. Feng, G. Lu and X. Huang, Polymer, 2015, **64**, 268-276.
32. X. Jiang, C. Feng, G. Lu and X. Huang, *ACS Macro Letters*, 2014, **3 (11)**, 1121-1125.
33. T. S. Kale, A. Klaikherd, B. Popere, S. Thayumanavan, *Langmuir*, 2009, **25 (17)**, 9660-9670.
34. C. Feng, G. Lu, Y. Li, X. Huang, *Langmuir*, 2013, **29 (34)**, 10922-10931.
35. S. R. Mane, N, V. Rao and R. Shunmugam, *ACS Macro Lett.*, 2012, **1 (4)**, 482-488.
36. W.-K. Miao, Y.-K. Yan, X.-L. Wang, Y. Xiao, L.-J. Ren, P. Zheng, C.-H. Wang, L.-X. Ren, W. Wang, *ACS Macro Lett.*, 2014, **3 (2)**, 211-215.
37. Y. Zhu, L. Liu and J. Du, *Macromolecules*, 2012, **46 (1)**, 194-203.
38. H. Cui, Z. Chen, S. Zhong, K. L. Wooley, D. J. Pochan, *Science*, 2007, **317 (5838)**, 647-650.
39. R. C. Hayward and D. J. Pochan, *Macromolecules*, 2010, **43 (8)**, 3577-3584.
40. J. N. Israelachvili, D. J. Mitchell and B. W. Ninham, *Biochimica et Biophysica Acta (BBA)-Biomembranes*, 1977, **470 (2)**, 185-201.
41. L. Zhang and A. Eisenberg, *J. Am. Chem. Soc.*, 1996, **118 (13)**, 3168-3181.
42. Y. Avlasevich, C. Li and K. Müllen, *J. Mater. Chem.*, 2010, **20 (34)**, 3814-3826.
43. D. Yao, T. P. Bender, P. J. Gerroir, P. R. Sundararajan, *Macromolecules*, 2005, **38 (16)**, 6972-6978.
44. C. Y. Hsu, S. C. Chang, K. Y. Hsu, Y. L. Liu, *Macromol. Rapid Commun.*, 2013, **34 (8)**, 689-694.
45. M. Yin, J. Shen, W. Pisula, M. Liang, L. Zhi, K. Müllen, *J. Am. Chem. Soc.*, 2009, **131 (41)**, 14618-14619.
46. J. Zhang, S. You, S. Yan, K. Müllen, W. Yang, M. Yin, *Chem. Commun.*, 2014, **50 (57)**, 7511-7513
47. J. Chiefari, Y. Chong, F. Ercole, J. Krstina, J. Jeffery, T. P. Le, R. T. Mayadunne, G. F. Meijs, C. L. Moad, G. Moad, *Macromolecules*, 1998, **31 (16)**, 5559-5562.
48. S. Perrier and P. Takolpuckdee, *J. Polym. Sci., Part A: Polym. Chem.*, 2005, **43 (22)**, 5347-5393.
49. G. Moad, Y. Chong, A. Postma, E. Rizzardo, S. H. Thang, *Polymer*, 2005, **46 (19)**, 8458-8468.
50. H. Willcock and R. K. O'Reilly, *Poly. Chem.*, 2010, **1 (2)**, 149-157.
51.
52. A. O. Moughton and R. K. O'Reilly, *Chem. Commun.*, 2010, **46 (7)**, 1091-1093.
53. J. Xu, L. Tao, C. Boyer, A. B. Lowe, T. P. Davis, *Macromolecules*, 2010, **44 (2)**, 299-312.
54. J. Du, H. Willcock, J. P. Patterson, I. Portman, R. K. O'Reilly, *Small*, 2011, **7 (14)**, 2070-2080.\
55. B. He, Y. Chu, M. Yin, K. Müllen, C. An, J. Shen, *Adv. Mater.*, 2013, **25 (33)**, 4580-4584.

56. R. Haag, J.-F. Stumbé, A. Sunder, H. Frey, A. Hebel, *Macromolecules*, 2000, **33 (22)**, 8158-8166.
57. Y. Lin, X. Liu, Z. Dong, B. Li, X. Chen, Y.-S. Li, *Biomacromolecules*, 2008, **9 (10)**, 2629-2636.
58. R. K. Kainthan, C. Mugabe, H. M. Burt, D. E. Brooks, *Biomacromolecules*, 2008, **9 (3)**, 886-895.
59. K. Ranganathan, R. Deng, R. K. Kainthan, C. Wu, D. E. Brooks, J. N. Kizhakkedathu, *Macromolecules*, 2008, **41 (12)**, 4226-4234.
60. R. K. Kainthan, D. E. Brooks, *Bioconjugate Chem.*, 2008, **19 (11)**, 2231-2238.
61. D. Liu, S. D. Feyter, M. Cotlet, U.-M. Wiesler, T. Weil, A. Herrmann, K. Müllen, F. C. De Schryver, *Macromolecules*, 2003, **36 (22)**, 8489-8498.
62. K. Aoi, T. Hatanaka, K. Tsutsumiuchi, M. Okada, T. Imae, *Macromol. Rapid Commun*., 1999, **20 (7)**, 378-382.
63. D.Kannaiyan and T. Imae, *Langmuir*, 2009, **25 (9)**, 5282-5285.
64. X. Liu, B. He, Z. Xu, M. Yin, W. Yang, H. Zhang, J. Cao, J. Shen, *Nanoscale*, 2015, **7(2)**, 445-449
65. I. Bányai, M. Kéri, Z. Nagy, M. Berka, L. P. Balogh, *Soft Matter*, 2013, **9 (5)**, 1645-1655.
66. I. Suarez, R. Rosal, A. Rodriguez, A. Ucles, A. Fernandez-Alba, M. Hernando, E. García-Calvo, *TrAC Trends Anal. Chem.*, 2011, **30 (3)**, 492-506.
67. S. Wang, J. Zhu, M. Shen, M. Zhu, X. Shi, *ACS applied mater. Inter.*, 2014, **6 (3)**, 2153-2161.
68. W.-I. Hung, C.-H. Chang, Y.-H. Chang, P.-S. Wu, C.-B. Hung, K.-C. Chang, M.-C. Lai, S.-C. Hsu, Y. Wei, X.-R. Jia, *Langmuir*, 2013, **29 (39)**, 12075-12083.
69. R. C. Hedden and B. J.Bauer, *Macromolecules*, 2003, **36 (6)**, 1829-1835.
70. L. Jiang, L. Ding, B. He, J. Shen, Z. Xu, M. Yin, X. Zhang, *Nanoscale*, 2014, **6 (17)**, 9965-9969.
71. Z. Xu, B. He, W. Wei, K. Liu, M. Yin, W. Yang, J. Shen, *J. Mater. Chem. B*, 2014, **2 (20**), 3079-3086.
72. Z. Xu, B. He, J. Shen, W. Yang, M. Yin, *Chem. Commun*., 2013, **49 (35)**, 3646-3648.
73. V. Atanasov, V. Sinigersky, M. Klapper, K. Müllen, *Macromolecules*, 2005, **38 (5)**, 1672-1683.
74. K. W. Chooi, A. I. Gray, L. Tetley, Y. Fan, I. F. Uchegbu, *Langmuir*, 2009, **26 (4)**, 2301-2316.
75. C. A. Nijhuis, J. K. Sinha, G. Wittstock, J. Huskens, B. J. Ravoo, D. N. Reinhoudt, *Langmuir*, 2006, **22 (23)**, 9770-9775.
76. X. Qu, L. Omar, T. B. H. Le, L. Tetley, K. Bolton, K. W. Chooi, W. Wang, I. F. Uchegbu, *Langmuir*, 2008, **24 (18)**, 9997-10004.
77. M. Yin, N. Kang, G. Cui, Z. Liu, F. Wang, W. Yang, M. Klapper, K. Müllen, *Chem.-Eur. J.*, 2012, **18 (8)**, 2239-2243.
78. S. You, Q. Cai, K. Müllen, W. Yang, M. Yin, *Chem. Commun.*, 2014, **50 (7)**, 823-825.
79. M. Yin, C. Feng, J. Shen, Y. Yu, Z. Xu, W. Yang, W. Knoll, K .Müllen, *Small*, 2011, **7 (12)**, 1629-1634.
80. G. I. Mashanov, T. A. Nenasheva, M. Peckham, J. E. Molloy, *Biochem. Soc. Trans*., 2006, **34 (5)**, 983-988.
81. V. Vukojevic´, A. Pramanik, T. Yakovleva, R. Rigler, L. Terenius, G. Bakalkin, *Cell. Mol. Life Sci.*, 2005, **62 (5)**, 535-550.
82. L. D. Lavis, T. Y. Chao, R. T. Raines, *ACS Chem. Biol*., 2006, **1 (4)**, 252-260.
83. I. L. Medintz, H. T. Uyeda, E. R. Goldman, H. Mattoussi, *Nat. Mater.*, 2005, **4 (6)**, 435-446.
84. R. P. Kulkarni, D. D. Wu, M. E. Davis, S. E. Fraser, *Proc. Natl. Acad. Sci. U.S.A.*, 2005, **102 (21)**, 7523-7528.
85. P. M.Viallet, T. Vo-Dinh, *Curr. Protein Pept. Sci.*, 2003, **4 (5)**, 375-388.
86. J. K. Jaiswal, S. M. Simon, *Nat. Chem. Biol.*, 2007, **3 (2)**, 92-98.
87. M. R. Gwinn, V. Vallyathan, *Environ. Health Perspect.*, 2006, **12 (114)**, 1818-1825.
88. D. A. Groneberg, M. Giersig, T. Welte, U. Pison, *Curr. Drug Targets*, 2006, **6 (7)**, 643-648.
89. M. Yin, C. R. Kuhlmann, K. Sorokina, C. Li, G. Mihov, E. Pietrowski, K. Koynov, M. Klapper, H. J. Luhmann, T. Weil, *Biomacromolecules*, 2008, **9 (5)**, 1381-1389.
90. S. K. Yang, X. Shi, S. Park, S. Doganay, T. Ha, S. C. Zimmerman, *J. Am. Chem. Soc.*, 2011, **133 (49)**, 9964-9967.
91. C. L. Feng, M. Yin, D. Zhang, S. Zhu, A. M. Caminade, J. P. Majoral, K. Müllen, *Macromol. Rapid Commun.*, 2011, **32 (8)**, 679-683.
92. D. H. Dube and C. R. Bertozzi, *Nat. Rev. Drug Discov*., 2005, **4 (15)**, 477-488.
93. L. Calzolai, F. Franchini, D. Gilliland and F. Rossi, *Nano Lett.*, 2010, **10 (45)**, 3101-3105.
94. J. T. Hyotyla, J. Deng and R. Y. Lim, *ACS Nano*, 2011, **5 (43)**, 5180-5187.
95. Z. I. Watts and C. J. Easton, *J. Am. Chem. Soc.*, 2009, **131 (89)**, 11323-11325.
96. C. Phillips, L. R. Roberts, M. Schade, R. Bazin, A. Bent, N. L. Davies, R. Moore, A. D. Pannifer, A. R. Pickford, S. H. Prior, *J. Am. Chem. Soc.*, 2011, **133 (47)**, 9696-9699.
97. M. Yin, J. Shen, G. O. Pflugfelder, K. Müllen, *J. Am. Chem. Soc.*, 2008, **130 (25)**, 7806-7807.
98. M. Yin, J. Shen, R. Gropeanu, G. O. Pflugfelder, T. Weil, K. Müllen, *Small*, 2008, **4 (7)**, 894-898.
99. B. S. Sandanaraj, R. Demont and S. Thayumanavan, J. *Am. Chem. Soc.*, 2007, **129 (12)**, 3506-3507.
100. S. Ghosh, V. Yesilyurt, E. N. Savariar, K. Irvin, S. Thayumanavan, *J. Polym. Sci., Part A: Polym. Chem.*, 2009, **47 (4)**, 1052-1060.
101. M. Y. Combariza, E. N. Savariar, D. R. Vutukuri, S. Thayumanavan, R. W. Vachet, *Anal. Chem.*, 2007, **79 (18)**, 7124-7130.
102. S. Wan, Y. Zheng, J. Shen, W. Yang, M. Yin, *ACS applied mater. Inter.*, **6(22)**, 19515-19519.
103. A. Sassolas, B. D. Leca-Bouvier and L. J. Blum, *Chem. Rev.*, 2008, **108 (1)**, 109-139.
104. R. Benters, C. Niemeyer and D. Wöhrle, *Chem. Bio. Chem.*, 2001, **2 (9)**, 686-694.
105. D. R. Kauffman and A. Star, *Chem. Soc. Rev.*, 2008, **37 (6)**, 1197-1206.
106. M. Yin, K. Ding, R. A. Gropeanu, J. Shen, R. D. Berger, T. Weil, K. Müllen, *Bio macromolecules*, 2008, **9 (11)**, 3231-3238.
107. Y. Yu, M. Yin, K. Müllen, W. Knoll, *J. Mater. Chem.*, 2012, **22 (16)**, 7880-7886.
108. K. Liu, Z. Xu, M. Yin, W. Yang, B. He, W. Wei, J. Shen, *J. Mater. Chem. B*, 2014, **2 (15**), 2093-2096.
109. C. M. Raynaud, J. Hernandez, F. P. Llorca, P. Nuciforo, M. C. Mathieu, F. Commo, S. Delaloge, L. Sabatier, F. Andre, J. Soria, *J. Am. J. Clin. Oncol.* 2010, **33**, 341-350.
110. D. X. Shen, F. Zhou, Z. Xu, B. He, M. Li, J. Shen, M. Yin, C. An, *J. Mater. Chem. B*, 2014, **2 (29**), 4653-4659.
111. T. Sun, Y. S. Zhang, B. Pang, D. C. Hyun, M. Yang and Y. Xia, *Angew. Chem. Int. Ed.*, 2014, **53 (79)**, 12320-12364.
112. B. Städler, A. D. Price and A. N. Zelikin, *Adv. Funct. Mater.*, 2011, **21 (1)**, 14-28.
113. Y. Li, G. H. Gao and D. S. Lee, *Adv. Healthc. Mater*., 2013, **2(3)**, 388-417.
114. M. H. Stenzel, *Chem. Commun.*, 2008, **43 (30)**, 3486-3503.
115. C. Gao, Y. Wang, W. Zhu, Z. Shen, *Chinese J. Polym. Sci.*, 2014, **32(11)**, 1431-1441.
116. S. R. Mane, N, V. Rao, K. Chaterjee, H. Dinda, S. Nag, A. Kishore, J. Das Sarma, R. Shunmugam, *Macromolecules*, 2012, **45 (19)**, 8037-8042.
117. L. Fan, H. Lu, K. Zou, J. Chen, J. Du, *Chem. Commun.*, 2013, **49 (98)**, 11521-11523.
118. E. K. Lim, Y. M. Huh, J. Yang, K. Lee, J. S. Suh and S. Haam, *Adv. Mater.*, 2011, **23 (29)**, 2436-2442.
119. D. J. Keddie, G. Moad, E. Rizzardo and S. H. Thang, *Macromolecules*, 2012, **45 (25)**, 5321-5342.